land

MDPI

Article

Monitoring Sustainable Development Goal Indicator 15.3.1 on Land Degradation Using SEPAL: Examples, Challenges and Prospects

Amit Ghosh [1,*], Pierrick Rambaud [1], Yelena Finegold [1], Inge Jonckheere [1], Pablo Martin-Ortega [1], Rashed Jalal [1], Adebowale Daniel Adebayo [2], Ana Alvarez [3], Martin Borretti [3], Jose Caela [4], Tuhin Ghosh [5], Erik Lindquist [1] and Matieu Henry [1]

[1] Food and Agriculture Organization of the United Nations, 00153 Rome, Italy; pierrick.rambaud@fao.org (P.R.); yelena.finegold@fao.org (Y.F.); inge.jonckheere@fao.org (I.J.); pablo.martin@fao.org (P.M.-O.); rashed.jalal@fao.org (R.J.); erik.lindquist@fao.org (E.L.); matieu.henry@fao.org (M.H.)
[2] Department of Geographical Science, University of Maryland, College Park, MD 20742, USA; adadebay@umd.edu
[3] Ministerio de Vivienda y Ordenamiento Territorial, Montevideo 11000, Uruguay; anaalvarez@mvot.gub.uy (A.A.); mborretti@mvot.gub.uy (M.B.)
[4] Food and Agriculture Organization of the United Nations, Huambo 298, Angola; jose.caela@fao.org
[5] School of Oceanographic Studies, Jadavpur University, Kolkata 700032, India; tuhin.ghosh@jadavpuruniversity.in
* Correspondence: amit.ghosh@fao.org

Abstract: A third of the world's ecosystems are considered degraded, and there is an urgent need for protection and restoration to make the planet healthier. The Sustainable Development Goals (SDGs) target 15.3 aims at protecting and restoring the terrestrial ecosystem to achieve a land degradation-neutral world by 2030. Land restoration through inclusive and productive growth is indispensable to promote sustainable development by fostering climate change-resistant, poverty-alleviating, and environmentally protective economic growth. The SDG Indicator 15.3.1 is used to measure progress towards a land degradation-neutral world. Earth observation datasets are the primary data sources for deriving the three sub-indicators of indicator 15.3.1. It requires selecting, querying, and processing a substantial historical archive of data. To reduce the complexities, make the calculation user-friendly, and adapt it to in-country applications, a module on the FAO's SEPAL platform has been developed in compliance with the UNCCD Good Practice Guidance (GPG v2) to derive the necessary statistics and maps for monitoring and reporting land degradation. The module uses satellite data from Landsat, Sentinel 2, and MODIS sensors for primary productivity assessment, along with other datasets enabling high-resolution to large-scale assessment of land degradation. The use of an in-country land cover transition matrix along with in-country land cover data enables a more accurate assessment of land cover changes over time. Four different case studies from Bangladesh, Nigeria, Uruguay, and Angola are presented to highlight the prospect and challenges of monitoring land degradation using various datasets, including LCML-based national land cover legend and land cover data.

Keywords: remote sensing; land cover; land cover meta language; cloud computing; sustainable land management

Citation: Ghosh, A.; Rambaud, P.; Finegold, Y.; Jonckheere, I.; Martin-Ortega, P.; Jalal, R.; Adebayo, A.D.; Alvarez, A.; Borretti, M.; Caela, J.; et al. Monitoring Sustainable Development Goal Indicator 15.3.1 on Land Degradation Using SEPAL: Examples, Challenges and Prospects. *Land* **2024**, *13*, 1027. https://doi.org/10.3390/land13071027

Academic Editor: Elias Symeonakis

Received: 13 May 2024
Revised: 1 July 2024
Accepted: 4 July 2024
Published: 9 July 2024

1. Introduction

Land degradation is defined as a process that reduces the current or potential capability of the land to produce goods or services. It can be caused by natural or human-induced factors, such as water erosion, salinization, compaction, waterlogging, deforestation, overgrazing, etc. [1]. Based on estimates, 34 percent of pasture and cropland are affected by degradation brought on by humans [2]. An estimated 24 billion metric tons of fertile soil

is lost annually, primarily as a result of unsustainable agricultural practices [3]. About 25 percent of the total land area has been degraded due to anthropogenic causes that are also contributing to climate change through the release of soil carbon and nitrous oxide into the atmosphere [4]. If this trend of degradation continues, about 95 percent of the Earth's land areas could become degraded by 2050 [3]. According to the United Nations Convention to Combat Desertification (UNCCD), land degradation affects about 1.5 billion people [5]. Therefore, monitoring and assessing land degradation is essential for developing effective strategies and policies to combat further degradation and restore the already degraded land. UNCCD introduced Land Degradation Neutrality (LDN) to combat land degradation. It is a state in which the quantity and quality of land resources necessary to support ecosystem functions and services remain stable or increase at a given spatial and temporal scale [6]. So, land restoration through inclusive and productive growth promotes sustainable development by fostering climate change-resistant, poverty-alleviating, and environmentally protective economic growth [7]. The UN Decade on Ecosystem Restoration is another notable recent initiative that promotes restoration as a nature-based solution for the safeguarding and restoration of ecosystems worldwide [8].

LDN is a key component of Sustainable Development Goals (SDGs) target 15.3, which aims at protecting and restoring the terrestrial ecosystem to achieve a land degradation-neutral world by 2030. Indicator 15.3.1 (proportion of degraded land over total land area) is used to measure progress towards LDN. It has three sub-indicators: (i) Land productivity; (ii) Land cover and land cover change; (iii) Carbon stocks above and below ground [9].

Earth observation and geospatial techniques offer valuable tools and data for mapping, assessing, and monitoring land degradation [10]. Earth observation data have been widely used to monitor land productivity dynamics at different spatial and temporal resolutions, from local to global scales and from daily to decadal time steps [11]. Satellite data provide timely, accurate, and reliable information on the biophysical and spectral characteristics of the land surface, which can be used to detect and quantify different types of land degradation [12]. Various methods and approaches have been developed to analyse remote sensing and earth observation data for detecting, quantifying, and modelling land productivity dynamics and land cover changes [13,14]. For example, trend analysis methods can identify the direction and magnitude of land productivity changes over time, breakpoint detection methods can detect abrupt changes or shifts in land productivity time series, machine learning methods can model the relationships between land productivity and its driving factors, and forecasting methods can predict the future scenarios of land productivity under different climate and land use conditions [15]. Biophysical variables such as vegetation indices are common indicators used to monitor the trend in land productivity. It is a measure of vegetation greenness and photosynthetic activity that has been shown to be related to biophysical variables that control vegetation productivity and land/atmosphere fluxes [16]. On the other hand, GIS techniques enable the integration and analysis of multiple data sources, such as remote sensing images, digital elevation models (DEMs), soil maps, climate data, etc., to identify the causes, drivers, and impacts of land degradation [17].

However, there are still challenges in using suitable information for reporting land degradation or restoration. The use of newly available technologies and data allows for the preparation of information at high spatial resolution and has the potential to combine the use of geographic information for reporting and planning land degradation and restoration. Recently available Sentinel and Landsat satellite imageries, as well as NICFI planet data, offer the potential to bring cost-efficient solutions for tracking and implementing sustainable land management and land restoration in general. On the other hand, technological progress in cloud computing, big data, and advanced algorithms provides efficient solutions within a relatively short period of time.

The objective of the article is to present a cloud-based module on the SEPAL cloud computing platform to prepare data and information for monitoring and reporting the Sustainable Development Goals (SDGs) target 15.3 using different input data and methods and to understand the opportunities and challenges of using country-specific information.

Earth observation datasets are the primary sources of data for deriving these sub-indicators. It requires selecting, querying, and processing a substantial historical archive of data to derive the information for the sub-indicators. This module on the SEPAL platform has been developed in compliance with the UNCCD Good Practice Guidance (GPG v2 [18]) to remove the complexities in deriving all the necessary statistics and maps for reporting by the relevant stakeholders.

2. Materials and Methods

2.1. The SEPAL Cloud Computing Platform

SEPAL is a cloud-computing-based platform for geospatial data analysis with a focus on querying, processing, and building advanced analytic solutions using earth observation data. It contains all the major open-source geospatial tools and libraries. The platform can be accessed at https://sepal.io (accessed on 12 May 2024). It is an open platform anyone can use after registering to it. It provides cloud computing facilities from small to very large-scale analysis using the cloud infrastructure. The four important navigation buttons are Process, Files, Terminal and Apps.

Process

The process tab provides a set of recipes to query and process satellite data for geospatial analyses. With recipes, an user can access the multi-petabyte catalog of satellite imagery from Google Earth Engine using easy-to-follow steps and a useful set of parameters and options.

Files

Files is a simple file manager to manage the directories and files stored in the user's personal SEPAL storage folder. Data and information are stored in the SEPAL storage for analysis and processing using SEPAL's recipes, modules, and tools.

Terminal

Terminal provides access to the command-line interface from the instances of Ubuntu-based GNU/Linux cloud computers. This command-line interface can be used in a variety of ways to process and manage data using a set of open-source software, such as Geospatial Data Abstraction Library (GDAL, version 3.8.4) [19], Orfeo ToolBox (OTB, version 8.1.2) [20], GuidosToolbox Workbench (GWB, version 1.9.0) [21], and Open Foris Geospatial Toolkit (OFGT, version 1.25.4) [22] etc. A large instance in terms of CPU and RAM can be used to process big data, which is not possible in a personal computer. This is one of the advantages of the platform that enables users to perform sophisticated data analysis with complex hardware and software setups.

Apps

Apps provides a collection of preloaded applications for performing specific tasks. It also includes tools like R Studio and Jupyter Notebook and Jupyter Labs for programming and scripting. The SDG module 15.3.1 is available in this section.

2.2. Sepal 15.3.1 Module

2.2.1. Building Block

The SDG indicator module uses the Python API of Google Earth Engine [23] and SEPAL's UI framework-based frontend (Figure 1). The module performs the calculation of high volume of satellite and other data in the Google Earth Engine, and the post processing of the data is performed inside the app instance. The module is designed to provide multiple option settings, from selection of the input data to the choice of indicators and parameters, using an easy-to-use graphical user interface. This facilitates the users needs and integration into the existing national frameworks for land degradation monitoring. For example, the inclusion of Landsat and Sentinel 2 data makes it possible to investigate the local context at high resolution, whereas MODIS is suitable for assessment at the national scale. The module also allows users to use in-country land cover data to compute the land

cover change sub-indicator. The following section presents the methodologies adopted in the module, including the source of the default data set.

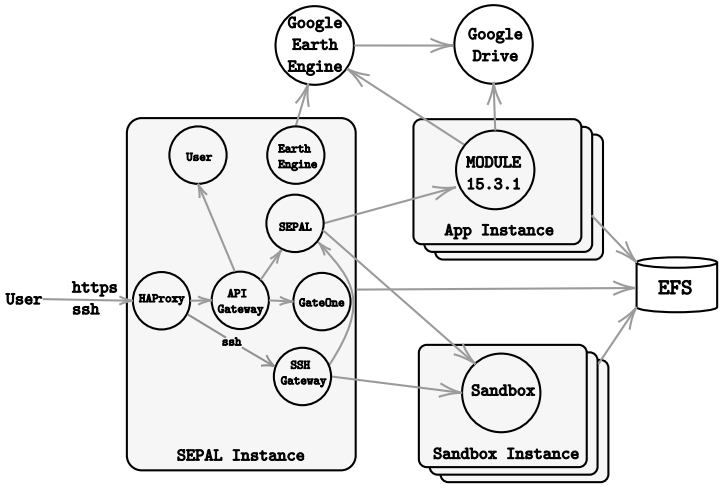

Figure 1. A simplified structure of the SEPAL's work flows for Google-Earth-Engine-based modules (based on the SEPAL's architecture diagram [24]).

2.2.2. Methodology

The second version of UNCCD Good Practice Guidance (GPG v2) provides guidance on how to calculate the extent of land degradation for reporting on the indicator 15.3.1 [18]. The methodologies implemented in the module are in line with this GPG v2.

The nature of land degradation is complex, and it is a multifaceted phenomenon that needs a comprehensive assessment [25]. A single source of information is not enough to accurately capture the full extent of land degradation [26]. The SDG indicator 15.3.1 uses three sub indicators: land cover and land cover change sub-indicator, land productivity sub-indicator, and carbon stocks above and below ground (Figure 2) [9,27]. Any area where one or more of the sub-indicators indicate that there has been land degradation is considered degraded land.

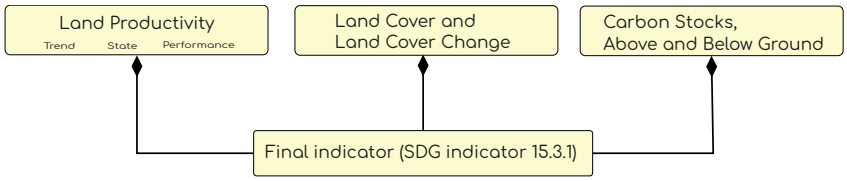

Figure 2. The three sub-indicators of the indicator 15.3.1.

2.2.3. Land Productivity Sub-Indicator

Land productivity refers to the amount of net primary production per unit of land and time. Changes in land productivity can provide insights into the decline or degradation of land as well as the restoration of land. The land productivity sub-indicator measures the changes in vegetation growth and biomass over time [28]. A continuous decrease in land productivity for a long time indicates potential land degradation. This sub-indicator is used to assess the status and trends of land degradation and restoration. It is one of the main indicators for monitoring and reporting the progress of Sustainable Development Goal 15.3.

The GPG proposes three matrices to detect such changes in land productivity, similar to the World Desertification Atlas [18,28,29]. These are productivity trend, productivity state, and productivity performance.

Remote sensing data serves as the primary source for land productivity monitoring and can provide consistent, spatially explicit, and timely information at various scales. We use vegetation indices as a proxy for land productivity because they offer a good approximation of NPP, accounting only for changes in productivity over time. The SEPAL module provides access to coarser to medium-resolution satellite data for three different vegetation indices (Table 1). Normalised Different Vegetation Index (NDVI) is the default, as proposed by GEO LDN initiatives [18,30]. The Enhanced Vegetation Index 2 (EVI2) can be considered for regions with high biomass, whereas the Modified Soil-adjusted Vegetation Index (MSVI) can be used for regions with low biomass, such as rangeland [31,32]. Vegetation indices are integrated to capture the growing seasons at the annual time series that is used to detect the changes in land productivity, with options to use the default annual integration, rain use efficiency model, or residual trend model [33–35]. The module also provides the option to select a threshold to define the growing seasons.

Productivity trend: The Mann–Kendall non-parametric trend analysis is used to describe the monotonic trend or trajectory (increasing or decreasing) of productivity for a given time period [36]. The z-score is used that quantifies the deviation of an annual value from the mean of the assessment period in terms of standard deviations to make sure the level of statistical confidence that the value is not solely due to chance [37]. The z score is categorised into three and five classes of different levels (Figure 3, Table 2).

Table 1. Available satellite dataset for land productivity assessment.

Satellite	Source	Temporal Coverage	Spatial Resolution
Landsat 4 (TM)	USGS/NASA	1982–1993	30 m
Landsat 5 (TM)	USGS/NASA	1984–2013	30 m
Landsat 7 (ETM+)	USGS/NASA	1999–2022	30 m
Landsat 8 (OLI)	USGS/NASA	2013–Present	30 m
Sentinel 2 (MSI)	ESA	2017–Present	10 m
MODIS (Aqua)	NASA	2002–Present	250 m
MODIS (Terra)	NASA	2000–Present	250 m
MODIS MOD17A3 (NPP)	NASA	2000–Present	500 m

Productivity state compares the mean annual values of the selected vegetation index over a three-year period with a long-term mean over a reference period as follows [18]:

$$\mu = \frac{\sum_{n-15}^{n-3} x_n}{13}, \tag{1}$$

$$\sigma = \sqrt{\frac{\sum_{n-15}^{n-3} (x_n - \mu)^2}{13}}, \tag{2}$$

where x is the productivity and n is the year of analysis.

The mean productivity of the current period is given as

$$\bar{x} = \frac{\sum_{n-2}^{n} x_n}{3}, \tag{3}$$

and the z score is given as

$$z = \frac{\bar{x} - \mu}{\frac{\sigma}{\sqrt{3}}}, \tag{4}$$

The ranges of z-values and corresponding categories are the same as those of the productivity trend (Figure 3, Table 2).

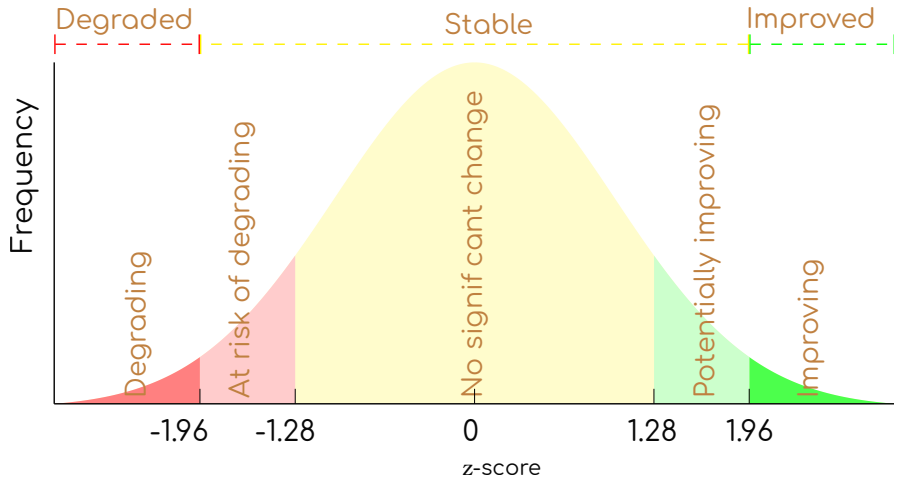

Figure 3. The scale and direction of productive trend and productivity state based on z score.

Table 2. Ranges of z-value and the corresponding classes of trend and state metrics.

z-Values	5 Level Classes	3 Level Classes
<-1.96	degrading	degraded
<-1.28 AND ≥ -1.96	Potentially degrading	Stable
≥ -1.28 AND ≤ 1.28	No significant change	Stable
> 1.28 AND ≤ 1.96	Potentially improving	Stable
> 1.96	Improving	Improved

Productivity performance indicates the level of local land productivity relative to other regions with similar productivity potential [18].

The Maximum Productivity Index NPP_{max} value (90th percentile) observed within the similar ecoregion is compared to the observed productivity value (observed NPP).

$$\text{performance} = \frac{NPP_{observed}}{NPP_{max}}, \tag{5}$$

The pixels with an NPP (vegetation index) less than 0.5 of the NPP_{max} are considered degraded. The module provides a list of datasets to define the regions with similar productivity potential; these are

- Global Agro-Environmental Stratification (GAES) [38];
- Historical agro-ecological zones (53 classes) from Global Agro Ecological Zones (GAEZ) [39];
- World Ecosystem [40];
- Global Homogeneous Response Units [41]; and
- A custom ecoregion based on default land cover data and soil texture.

These three metrics are combined to derive the productivity sub-indicator. There are two approaches mentioned in GPG v2 to combine the metrics. Figure 4 portrays the combination of both approaches–GPG v2 using solid colour lines and changes in GPG v1 using dashed lines to cut the over-emphasis of productivity degradation from declining trend alone. The three layers of circles represent the three different metrics.

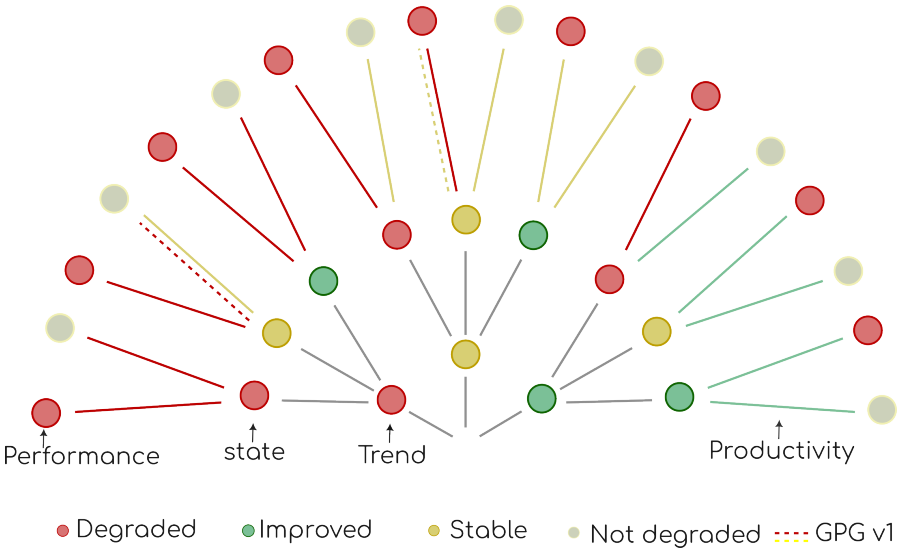

Figure 4. Possible combinations of the three metrics to get the productivity sub-indicators; dotted lines represent the combination initially proposed in GPG v1.

2.2.4. Land Cover and Land Cover Change Sub-Indicator

Land cover is the observed (bio) physical cover on the earth's surface [42]. In this context, land cover is used as a proxy for land use and land use change. Changes in land use clearly indicate the degradation and restoration of land.

The land cover sub-indicator is based on transitions of land cover from the initial year to the final year. It describes the nature of transition from one land cover to another. A transition matrix contains the transitions as degraded, stable, or improved. For example, conversion of forest land to grassland is considered degraded as it may result in soil erosion, biodiversity loss, and diminished carbon sequestration. The default matrix contains the UNCCD land cover categories and their transitions (Figure 5).

Figure 5. Interface of the default transition matrix that uses seven UNCCD land cover categories (D [red] = degraded, S [tan] = stable and I [green] = improved).

The default transitions can be altered based on local knowledge of land cover changes. However, the scope to implement all the important transitions is limited to these seven categories. A national land cover represents the most accurate and complex land cover classes in comparison to most of the global and regional land cover data [43,44]. Therefore, it is important to use national land cover data in combination with a customised land cover transition matrix. The module offers the ability to use national land cover data in combination with a customised land cover transition matrix. The customised matrix, A, needs to be in a proper format to use in the module:

$$\mathbf{A} = \begin{bmatrix} a_{11} & a_{12} & a_{13} & \cdots & a_{1n} \\ a_{21} & a_{22} & a_{23} & \cdots & a_{2n} \\ a_{31} & a_{32} & a_{33} & \cdots & a_{3n} \\ \vdots & \vdots & \vdots & \ddots & \vdots \\ a_{n1} & a_{n2} & a_{n3} & \cdots & a_{nn} \end{bmatrix}, \quad (6)$$

The first two columns, excluding the first two cells ($a_{31}...a_{n1}$and $a_{32}...a_{n2}$), contain class labels and pixel values for the initial land cover, respectively. The first two rows, excluding the first two cells, ($a_{13}...a_{1n}$and $a_{23}...a_{2n}$) contain class labels and pixel values for the final land cover, respectively. The other subset of the matrix,

$$\mathbf{B} = \begin{bmatrix} a_{33} & \cdots & a_{3n} \\ \vdots & \ddots & \vdots \\ 2_{n3} & \cdots & 3_{nn} \end{bmatrix}, \quad (7)$$

contain the main transition matrix. Cells $a_{11}, a_{12}, a_{21},$ and a_{22} are available to store some metadata. The value 1 to denote improved transitions, 0 for stable, and -1 for degraded transitions.

The European Space Agency Climate Change Initiative Land Cover (ESA CCI LC) dataset has been used as the default data source [45]. It provides consistent global annual land cover maps at 300 m spatial resolution from 1992 to 2022. Each pixel value corresponds to the label of a land cover class, which is defined based on the FAO Land Cover Classification System (LCCS) [42]. The module translates the classes into seven UNCCD broad land cover categories, as suggested in the GPG.

LCML-legend-based land cover data are more flexible and suitable for the land cover sub-indicator [18]. The use of the LCML-based legend expedites the process of generating an in-country land cover transition matrix. For example, the LCML-based legend can be automatically assessed to find the similarities between land cover classes [46]. Therefore, in-country land cover data can be used with a custom land cover transition matrix. FAO land cover registry provides access to the different global and national land cover legends for other countries to adapt the ISO standard (ISO 19144-2) on land cover [47,48].

In addition to module 15.3.1, SEPAL provides recipes to prepare optical and radar mosaics and land cover classification. The classification recipe supports LCML legend as input for land cover legend. Separate modules are also available for accuracy assessment and validation (https://docs.sepal.io/(accessed on 12 May 2024)).

2.2.5. Carbon Stocks, Above and Below Ground

Carbon stocks are the result of several processes that influence plant development and decomposition. These processes determine the changes in the amount of organic matter in terrestrial ecosystems [18]. Soil organic carbon (SOC) is the suggested metric where total terrestrial carbon stocks are not available. A reduction of 10% from the reference soil organic carbon (SOC) is classified as degraded.

The IPCC methodology to estimate change in SOC is used to account for changes in soil carbon stocks due to land use and land cover change [49]. The ESA CCI land cover is used to estimate the annual rate of change in carbon stock from the reference SOC stock from ISRIC. The method is based on the equation:

$$\Delta SOC = A \times \Delta C \times FLU \times FMG \times FI \quad (8)$$

where,

- ΔSOC is the annual change in SOC stock per unit area (t C ha^{-1} yr^{-1}),
- A is the area of land remaining in a land-use category or converted to another category (ha),
- ΔC is the annual rate of change in carbon stocks per unit area (t C ha^{-1} yr^{-1}),

- FLU is the stock change factor for land use or land-use change type,
- FMG is the stock change factor for management regime,
- FI is the stock change factor for input of organic matter.

2.2.6. Final Indicator

The one-out-all-out statistical principle is used to get the final state of land degradation from three sub-indicators (Figure 6). It shows how evidence from numerous sources comes together. So, the final layer shows degradation when any of the sub-indicator pixels in the same place capture degradation during the assessment time.

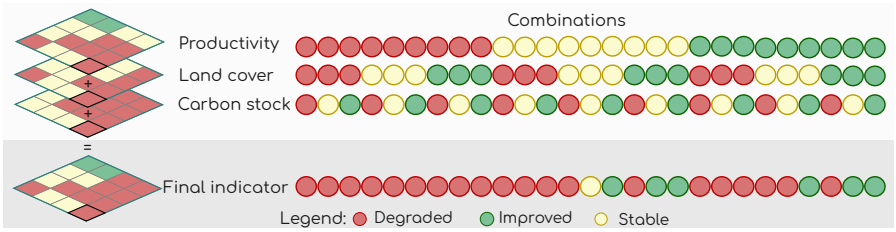

Figure 6. The complete set of combinations of three sub-indicators' statuses and the corresponding statuses of the final indicator.

3. Results

3.1. Interface

The interface of the module has been designed into four different widgets (Figure 7):

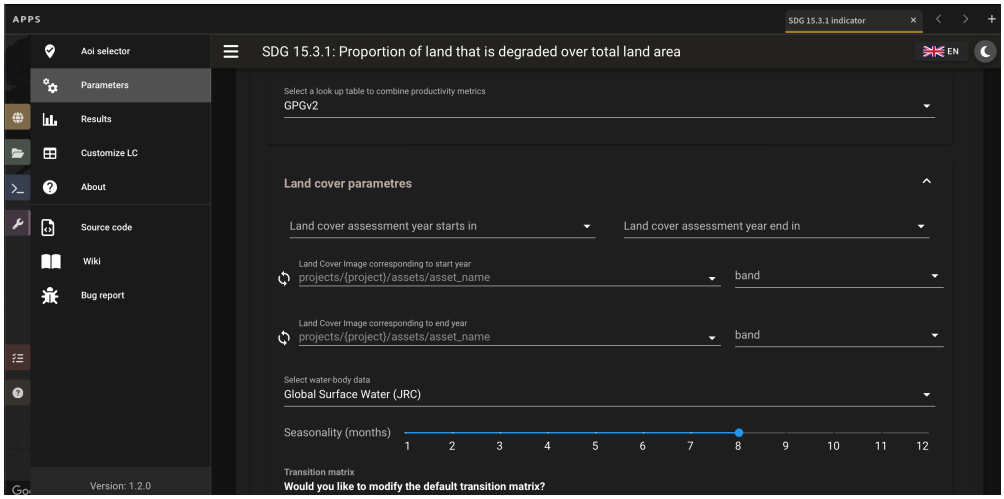

Figure 7. Different sections of SEPAL module 15.3.1's interface.

- Selection of area of interest—A range of options are available, from preloaded administrative boundaries to custom shapes.
- Selection of parameters—A wide range of input and specifications for each of the sub-indicators can be specified in this section. Most of the common parameters are set to the commonly used default values. More advance options are organised into three different sub-indicators under the advance options banner.
- Visualization and export of results —The results from the module that can be visualised and exported that consist of maps (raster data at sensors' resolution) of all the sub-indicators and productivity metrics;
- Customization of land cover categories/classes—This widget provides the functionality to reclassify/aggregate a land cover map to an UNCCD or a custom classification scheme.

3.2. Case Study 1: Large Scale Monitoring in Bangladesh and Nigeria

The methodology implemented in SEPAl 15.3.1 was piloted in part of Bangladesh and Nigera to test the performance in assessing the indicator in large areas.

3.2.1. Bangladesh

Two primary aspects characterising this country's physiography are a confined hilly region traversed by rivers and a deltaic plain that is affected by regular flooding. The major issues in terms of land degradation are the increase rate of deforestation, landslides, soil erosion, riverbank erosion, and intrusion of salinity [50]. The module has been tested in Cox's Bazar, where filed information on degradation and restoration was available [51]. This case study was intended to scale up the analysis to a larger area to test the performance of the module. The extent of land degradation in the area of interest was assessed using the global dataset for the baseline and reporting periods. The baseline period is assessment years against which changes in the recent years or reporting period are assessed. The GPG contains suggestions on the selection of reporting period, and the baseline period is fixed from 1 January 2000 to 31 December 2015. The main inputs for the assessment for the reporting period (2016–2022) and baseline period are the MODIS-based NDVI, GAEZ, ISRIC soil data, and ESA CCI land cover (Figure 8). Most of the degraded areas are located along rive courses and urbanised areas. Around 20 out of 64 districts are prone to riverbank erosion, which consumes around 8,700 hectares of land each year [52,53]. Therefore, changes in river routes and urbanisation are the main causes of degraded land in the area of interest (Figure 9).

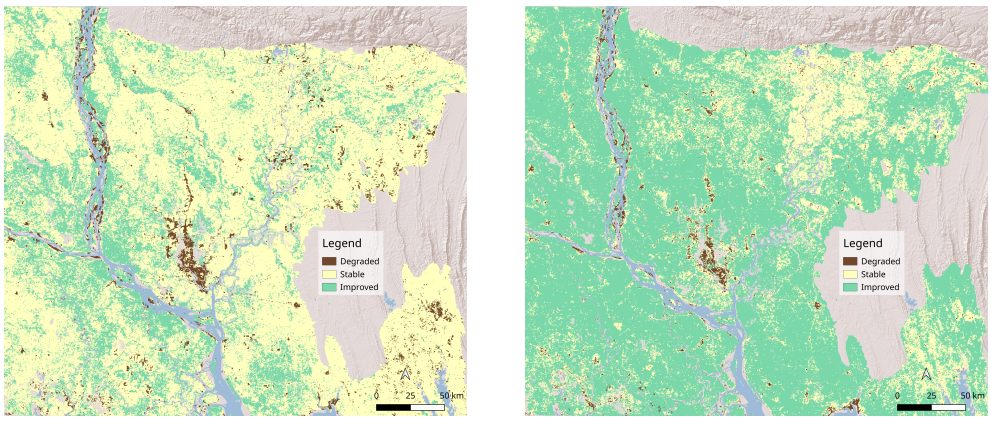

(**a**) Baseline status (**b**) Reporting status

Figure 8. Status of baseline and reporting status of the SDG indicator 15.3.1.

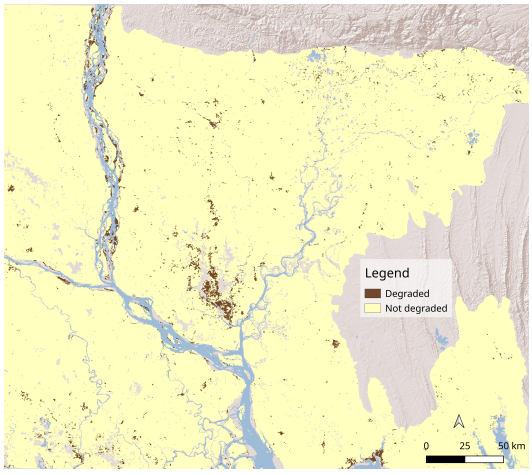

Figure 9. Final status of SDG indicator after combining the baseline and reporting status.

3.2.2. Nigeria

Land degradation in Nigeria is a pressing issue, with deforestation, soil erosion, and desertification having significant impacts on the country's agricultural productivity and food security [54]. The study considered two distinct vegetation indices, namely the Normalized Difference Vegetation Index (NDVI) and the Enhanced Vegetation Index 2 (EVI2), in order to compare the degradation extent seen during the reporting years spanning from 2012 to 2022. The degree of land degradation shown notable variations contingent upon the specific index employed for the assessment. The NDVI-based outcome exhibited a markedly greater degree of degradation during the reporting period in comparison to the EVI2-based outcome (Figure 10). In general, the results indicate that the selection of a vegetation index can exert a substantial influence on the extent of land degradation. A close inspection with high-resolution images suggests that the soil reflectance correction properties of the EVI2 tend to reduce the interannual variability of the vegetation signal in vegetation sparse regions. A thorough investigation is required to identify the underlying factors that are influencing the result.

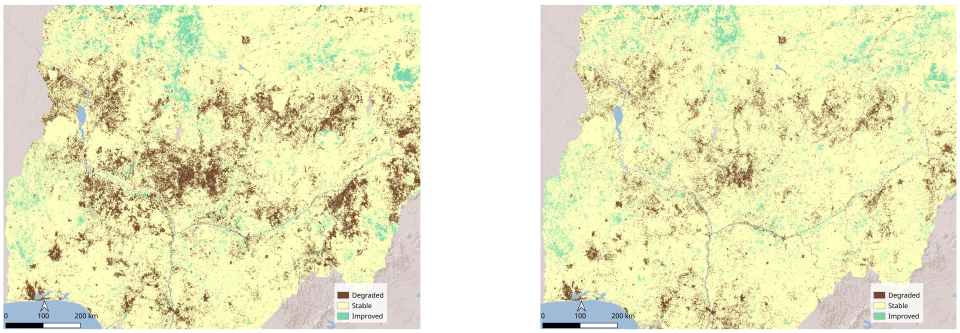

(**a**) NDVI-based land productivity (**b**) EVI-based land productivity

Figure 10. Extent of land degradation for reporting period using NDVI and EVI in Nigeria.

3.3. Case Study 2: Monitoring Land Degradation Status Using In-Country Land Cover Data in Uruguay

A comparative assessment of land degradation was conducted using ESA CCI and national land cover data to analyse the baseline period from 2000 to 2015. The LCML standard was used to prepare the national land cover data for both 2000 and 2015 [55]. There are 17 land cover classes that were used to prepare a national land cover transition matrix. One notable distinction between the national land cover transition matrix and the default land cover transition matrix lies in the segregation of native forests and exotic species plantations (primarily eucalyptus and pine) for timber production. In the national transition matrix, the latter exhibits a comparable pattern to that of crops. Conversely, in the default matrix, both classes were classified as belonging to the "tree cover area" class (Figure 11). The area of land forested in Uruguay for these purposes has had a substantial rise over the past three decades, contributing considerably to alterations in the country's land cover. At present, the extent of planted forest in Uruguay accounts for approximately six percent of the country's total land area, whilst the native forest encompasses less than five percent. From a soil degradation standpoint, it is evident that these two categories exhibit distinct behaviours. Consequently, it was decided to segregate these categories and consider forest plantations similar to 'crops'.

The primary factor contributing to variations in outcomes between the national land cover and the ESA CCI land cover data is the distinction between native forests and forest plantations, since the latter does not allow distinguishing one class from the other. Both classes are considered "tree cover". This is why the degraded area appears to be larger when using the national land cover dataset (Table 3). Conversely, the increase in forest plantations also leads to the emergence of large areas with enhanced productivity

(especially in the north of Uruguay) due to tree growth, as well as large areas with apparent loss of productivity, which occur when those forest plantations are harvested (Figure 12).

Land cover	2015	Plantación Forestal	Frutales	Cultivos Pequeños	Cultivos de Secano mayor a 4/5 ha	Cultivos Regados mayor a 4/5 ha	Bosque Nativo	Palmares	Campo Natural	Arbustos	Areas Naturalmente Inundables	Urbano Disperso	Equipamiento Urbano	Urbano	Minas, Areneras y Canteras	Suelo Desnudo	Aguas Artificales	Aguas Naturales
2000	Code	11	12	13	14	15	16	17	18	19	20	21	22	23	24	25	26	27
Plantación Forestal	11	0	0	0	0	0	1	1	1	1	1	-1	-1	-1	-1	-1	-1	-1
Frutales	12	0	0	0	0	0	1	1	1	1	1	-1	-1	-1	-1	-1	-1	-1
Cultivos Pequeños	13	0	0	0	0	0	1	1	1	1	1	-1	-1	-1	-1	-1	-1	-1
Cultivos de Secano mayor a 4/5 ha	14	0	0	0	0	0	1	1	1	1	1	-1	-1	-1	-1	-1	-1	-1
Cultivos Regados mayor a 4/5 ha	15	0	0	0	0	0	1	1	1	1	1	-1	-1	-1	-1	-1	-1	-1
Bosque Nativo	16	-1	-1	-1	-1	-1	0	0	-1	-1	0	-1	-1	-1	-1	-1	-1	-1
Palmares	17	-1	-1	-1	-1	-1	0	0	-1	-1	-1	-1	-1	-1	-1	-1	-1	-1
Campo Natural	18	-1	-1	-1	-1	-1	1	1	0	-1	0	-1	-1	-1	-1	-1	-1	-1
Arbustos	19	-1	-1	-1	-1	-1	1	1	1	0	0	-1	-1	-1	-1	-1	-1	-1
Areas Naturalmente Inundables	20	-1	-1	-1	-1	-1	0	0	0	0	0	-1	-1	-1	-1	-1	-1	-1
Urbano Disperso	21	1	1	1	1	1	1	1	1	1	1	0	-1	-1	-1	-1	-1	-1
Equipamiento Urbano	22	1	1	1	1	1	1	1	1	1	1	1	0	0	-1	1	0	1
Urbano	23	1	1	1	1	1	1	1	1	1	1	1	0	0	-1	1	0	1
Minas, Arenera y Canteras	24	1	1	1	1	1	1	1	1	1	1	1	1	1	0	1	0	1
Suelo Desnudo	25	1	1	1	1	1	1	1	1	1	1	-1	-1	-1	-1	0	0	1
Aguas Artificales	26	1	1	1	1	1	1	1	1	1	1	1	0	0	0	0	0	0
Aguas Naturales	27	1	1	1	1	1	1	1	1	1	1	1	-1	-1	-1	-1	0	0

Figure 11. National land cover transition matrix for Uruguay as per SEPAL SDG 15.3.1 specification.

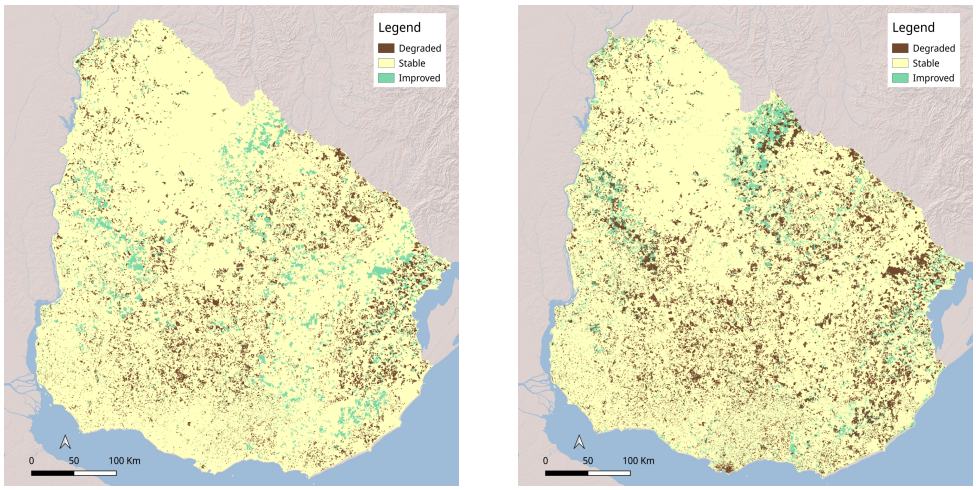

(**a**) (**b**)

Figure 12. Land cover sub-indicator indicator (15.3.1) for the baseline period. (**a**) Based on national custom transition matrix and national land cover data; (**b**) Based on the default transition matrix and ESA CCI land cover data.

Table 3. Land cover sub-indicator status during the baseline period in Uruguay using the ESA CCI and national land cover data (area in km^2).

Type of Land	National Land Cover Data	ESA CCI Land Cover
Degraded	25,015	13,547
Stable	139,877	129,333
Improved	9460	8517
Nodata	8112	1485
Total (Land)	174,352	151,397

3.4. Case Study 3: Comparison with MODIS and Landsat Sensors in Angola

This case study was conducted to support the FAO project "Sustainable Land Management in the target landscape of Central Angola". The goal was to use high resolution satellite data to identify the degradation hotspot for land restoration purposes. This assessment has been conducted for the baseline period (2001 to 2015) using Landsat and MODIS data to compare the results for Alto Hama commune in Huambo province, Angola. Apart from the different sensors, all the other parameters were the same for both analyses. Annual integration of NDVI from MODIS and Landsat 4, 5, 7, and 8 was used to prepare the

land productivity sub-indicator with the trend set to the original NDVI values. The look-up table from GPG v2 was used to combine the three productivity metrics. It was found that the MODIS-based vegetation indices are temporally consistent, whereas Landsat provides high spatial resolution. When compared to MODIS, Landsat provided more spatial details about degradation status (Figure 13). The Landsat-based analysis was able to capture four times more degraded land (17%) than the MODIS-based analysis (4%). A little less area of improved land was captured by Landsat-based analysis due to the missing part of Landsat 7 data. In summary, MODIS-based analysis captured fewer degraded areas than Landsat-based analysis, and in both analyses, stable land areas are the same (Table 4).

Table 4. Comparison of land degradation mapping using MODIS and Landsat satellite.

Sensor	Degraded [km^2, (%)]	Stable [km^2, (%)]	Improved [km^2, (%)]	Total [km^2]
Landsat	109, (17)	365, (57)	166, (26)	640
MODIS	26, (4)	377, (57)	237, (37)	640

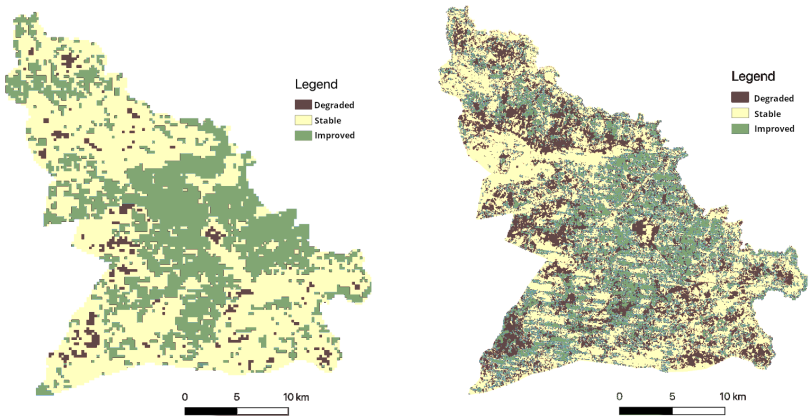

(**a**) Based on MODIS data (**b**) Based on Landsat data

Figure 13. Comparison of land degradation mapping using MODIS and Landsat satellite.

4. Discussion

Assessment of land degradation requires a set of datasets that are often large in terms of temporal and spatial dimensions. For example, assessment of land productivity for the baseline period requires 16 years of satellite data, and if high-resolution data are to be used, that poses challenges for data management, processing, and analysis. Big data requires high computational power, storage capacity, bandwidth, and software tools to deal with issues such as noise, outliers, uncertainty, and at the end calculation of the land productivity metrics. SEPAL provides an efficient cloud computing environment for large-scale processing and analysis of geospatial datasets without the need to set up a sophisticated computing environment. The case studies of Bangladesh and Nigeria are examples of such assessments where two different large geographies were considered.

Apart from the SDG module 15.3.1, the land cover classification module of SEPAL, along with other Open Foris tools, can be used to prepare in-country land cover datasets using country-specific legends, preferably LCML-based legends. The use of customized transition matrices enables local context specific analysis for each national reality. When compared to global data (e.g., ESA CCI land cover data), national land cover data provided more spatial details about degradation status. In summary, global land cover-based analysis captured fewer degraded areas than national land cover-based analysis. The case study of Uruguay is an example where SEPAL was used for the preparation and validation of recent land cover data and the indicator 15.3.1.

In the case of local-level assessment, the spatial resolution of remote sensing data determines the level of detail that can be observed and analyzed. Low spatial resolution data may not capture the heterogeneity and variability of land degradation processes and impacts. High spatial resolution data may provide more accurate and detailed information, but they are less available. Therefore, the option to use Landsat and Sentinel 2 for land productivity assessment is an advantage. However, in spite of a rich archive of high-resolution Landsat data, its narrow swath width causes sudden changes in values along the edges of the spatial mosaic and is limited by cloud cover, sensor failures, and data gaps. Land degradation is a dynamic and complex process that can vary over time due to natural and human factors. Also, limited temporal coverage of high resolution data does not provide enough information to capture the growing season properly. Therefore, temporal coverage is important to capture the changes and trends of land degradation and restoration.

Each type of degradation may have different indicators, drivers, and impacts. Therefore, it is challenging to develop a standardized methodology that can detect and quantify the type and cause of degradation using remote sensing data. Moreover, different regions may have different biophysical and socio-economic conditions that affect the definition and assessment of land degradation. The importance of selecting the most suitable index for accurate monitoring and reporting is also highlighted in the Nigeria case study. Therefore, it is important to use a suitable vegetation index considering the different factors involved. For example, EVI2 performs better in high biomass areas, whereas MSAVI performs better in rangeland areas. The assessment can be carried out separately for diverse geographies to apply a better-performing index for different ecological zones.

Another important challenge is the difficulty of detecting the type/cause of degradation using a standardized methodology and default global dataset. Several other indicators can be used to complement the result or for restoration of the degraded land using sustainable land management.

Moving forward, it will be crucial for policymakers and land managers to consider these differences in order to effectively combat land degradation and implement sustainable land management practices. Additionally, further research may be needed to better understand the factors influencing the discrepancies in results in order to improve future monitoring efforts. Validation of land degradation results is another area where further studies are required to formulate frameworks and methodologies, particularity for baseline status, as it detects degradation in the historical period.

Author Contributions: Conceptualization, A.G. and P.R.; methodology, A.G.; software, A.G. and P.R.; validation, Y.F., I.J., R.J. and P.M.-O.; formal analysis, A.G., A.A., M.B., J.C. and A.D.A.; writing—original draft preparation, A.G.; writing—review and editing, Y.F., I.J. and T.G.; visualization, A.G.; supervision, E.L. and M.H. All authors have read and agreed to the published version of the manuscript.

Funding: This research received no external funding.

Data Availability Statement: The source code of the module is available at : https://github.com/sepal-contrib/sdg_15.3.1 (accessed on 12 May 2024).

Acknowledgments: The authors would like to thank the anonymous reviewers for their comments and suggestion to improve the manuscript

Conflicts of Interest: The authors declare no conflicts of interest.

References

1. Baroudy, A.E. Monitoring land degradation using remote sensing and GIS techniques in an area of the middle Nile Delta, Egypt. *CATENA* **2011**, *87*, 201–208. [CrossRef]
2. FAO. *The State of the World's Land and Water Resources for Food and Agriculture—Systems at Breaking Point. Main Report*; FAO: Rome, Italy, 2022. [CrossRef]
3. IPBES. *The IPBES Assessment Report on Land Degradation and Restoration.*; Montanarella, L., Scholes, R., Brainich, A., Eds.; Secretariat of the Intergovernmental Science-Policy Platform on Biodiversity and Ecosystem Services: Bonn, Germany, 2018.

4. GEF. *Combating Land Degradation*; GEF: Washington, DC, USA, 2022.
5. UNCCD. *Desertification: The Invisible Frontline*, 2nd ed.; UNCCD: Bonn, Germany, 2014; Volume 214.
6. Kust, G.; Andreeva, O.; Cowie, A. Land Degradation Neutrality: Concept development, practical applications and assessment. *J. Environ. Manag.* **2017**, *195*, 16–24. [CrossRef] [PubMed]
7. Nelson, C.R.; Hallett, J.G.; Montoya, A.R.; Andrade, A.; Besacier, C.; Boerger, V.; Bouazza, K.; Chazdon, R.; Cohen-Shacham, E.; Danano, D.; et al. *Standards of Practice to Guide Ecosystem Restoration*; FAO: Rome, Italy, 2024. [CrossRef]
8. UN. United Nations Decade on Ecosystem Restoration (2021–2030). 2019. Available online: https://undocs.org/A/RES/73/284 (accessed on 10 February 2024).
9. UNCCD. *Scientific Conceptual Framework for Land Degradation Neutrality. A Report of the Science-Policy Interface*; Unccd-Spi Technical Series No. 01; UNCCD: Bonn, Germany, 2017.
10. Symeonakis, E. Land Degradation Assessment with Earth Observation. *Remote Sens.* **2022**, *14*, 1776. [CrossRef]
11. Koehler, J.; Kuenzer, C. Forecasting Spatio-Temporal Dynamics on the Land Surface Using Earth Observation Data—A Review. *Remote Sens.* **2020**, *12*, 3513. [CrossRef]
12. Lu, D.; Mausel, P.; Brondizio, E.; Moran, E. Change detection techniques. *Int. J. Remote Sens.* **2004**, *25*, 2365–2401. [CrossRef]
13. Kosmas, C.; Kairis, O.; Karavitis, C.; Ritsema, C.; Salvati, L.; Acikalin, S.; Alcalá, M.; Alfama, P.; Atlhopheng, J.; Barrera, J.; et al. Evaluation and Selection of Indicators for Land Degradation and Desertification Monitoring: Methodological Approach. *Environ. Manag.* **2014**, *54*, 951–970. [CrossRef] [PubMed]
14. Verburg, P.H.; van de Steeg, J.; Veldkamp, A.; Willemen, L. From land cover change to land function dynamics: A major challenge to improve land characterization. *J. Environ. Manag.* **2009**, *90*, 1327–1335. [CrossRef] [PubMed]
15. Wang, J.; Zhen, J.; Hu, W.; Chen, S.; Lizaga, I.; Zeraatpisheh, M.; Yang, X. Remote sensing of soil degradation: Progress and perspective. *Int. Soil Water Conserv. Res.* **2023**, *11*, 429–454. [CrossRef]
16. Hall, F.G.; Hilker, T.; Coops, N.C.; Lyapustin, A.; Huemmrich, K.F.; Middleton, E.; Margolis, H.; Drolet, G.; Black, T.A. Multi-angle remote sensing of forest light use efficiency by observing PRI variation with canopy shadow fraction. *Remote Sens. Environ.* **2008**, *112*, 3201–3211. [CrossRef]
17. Yang, X.; Zhang, X.; Lv, D.; Yin, S.; Zhang, M.; Zhu, Q.; Yu, Q.; Liu, B. Remote sensing estimation of the soil erosion cover-management factor for China's Loess Plateau. *Land Degrad. Dev.* **2020**, *31*, 1942–1955. [CrossRef]
18. Sims, N.; Green, C.; Newnham, G.; England, J.; Held, A.; Wulder, M.; Herold, M.; Cox, S.; Huete, A.; Kumar, L.; et al. Good Practice Guidance for SDG Indicator 15.3.1: Proportion of land that is degraded over total land area. In *United Nations Convention to Combat Desertification (UNCCD)*; Version 2.0; UNCCD: Bonn, Germany, 2021.
19. GDAL/OGR Contributors. *GDAL/OGR Geospatial Data Abstraction Software Library*; Open Source Geospatial Foundation: Beaverton, OR, USA, 2024.
20. Grizonnet, M.; Michel, J.; Poughon, V.; Inglada, J.; Savinaud, M.; Cresson, R. Orfeo ToolBox: Open source processing of remote sensing images. *Open Geospat. Data Softw. Stand.* **2017**, *2*, 15. [CrossRef]
21. Vogt, P.; Riitters, K.; Rambaud, P.; d'Annunzio, R.; Lindquist, E.; Pekkarinen, A. GuidosToolbox Workbench: Spatial analysis of raster maps for ecological applications. *Ecography* **2022**, *2022*, e05864. [CrossRef]
22. FAO. *Open Foris Geospatial Toolkit*; Food and Agriculture Organization of the United Nations: Rome, Italy, 2014.
23. Gorelick, N.; Hancher, M.; Dixon, M.; Ilyushchenko, S.; Thau, D.; Moore, R. Google Earth Engine: Planetary-scale geospatial analysis for everyone. *Remote Sens. Environ.* **2017**, *202*, 18–27. [CrossRef]
24. SEPAL Team. *SEPAL- System for Earth Observation Data Access, Processing and Analysis for Land Monitoring*; Food and Agriculture Organization of the United Nations: Rome, Italy, 2024. [CrossRef]
25. Chisholm, A.H.; Dumsday, R. *Land Degradation: Problems and Policies*; Cambridge University Press: Cambridge, UK, 1987.
26. Kairis, O.; Kosmas, C.; Karavitis, C.; Ritsema, C.; Salvati, L.; Acikalin, S.; Alcalá, M.; Alfama, P.; Atlhopheng, J.; Barrera, J.; et al. Evaluation and Selection of Indicators for Land Degradation and Desertification Monitoring: Types of Degradation, Causes, and Implications for Management. *Environ. Manag.* **2014**, *54*, 971–982. [CrossRef] [PubMed]
27. UNCCD. *Refinement of the Set of Impact Indicators on Strategic Objectives 1, 2 and 3*; Recommendations of the Ad Hoc Advisory Group of Technical Experts ICCD/COP(11)/CST/2; United Nations Convention to Combat Desertification (UNCCD): Bonn, Germany, 2013.
28. Ivits, E.; Cherlet, M. Land-productivity dynamics towards integrated assessment of land degradation at global scales. *Jt. Res. Cent. Eur. Comm.***2013**, *10*, 59315. [CrossRef]
29. Cherlet, M.; Hutchinson, C.; Reynolds, J.; Hill, J.; Sommer, S.; Von Maltitz, G. *World Atlas of Desertification*; Scientific Analysis or Review, Technical Guidance KJ-07-17-008-EN-C (Print), KJ-07-17-008-EN-N (Online); Joint Research Council: Luxembourg, 2018. [CrossRef]
30. Tucker, C.J. Red and photographic infrared linear combinations for monitoring vegetation. *Remote Sens. Environ.* **1979**, *8*, 127–150. [CrossRef]
31. Jiang, Z.; Huete, A.R.; Kim, Y.; Didan, K. 2-band enhanced vegetation index without a blue band and its application to AVHRR data. *Remote Sens. Model. Ecosyst. Sustain. IV SPIE* **2007**, 6679, 45–53.
32. Qi, J.; Chehbouni, A.; Huete, A.R.; Kerr, Y.H.; Sorooshian, S. A modified soil adjusted vegetation index. *Remote Sens. Environ.* **1994**, *48*, 119–126. [CrossRef]
33. Le Houérou, H.N. Rain use efficiency: A unifying concept in arid-land ecology. *J. Arid. Environ.* **1984**, *7*, 213–247. [CrossRef]

34. Evans, J.; Geerken, R. Discrimination between climate and human-induced dryland degradation. *J. Arid. Environ.* **2004**, *57*, 535–554. [CrossRef]
35. Wessels, K.J.; Prince, S.D.; Malherbe, J.; Small, J.; Frost, P.E.; VanZyl, D. A new approach to detect subtle land degradation and vegetation changes in semi-arid environments. *J. Arid. Environ.* **2007**, *70*, 722–737. [CrossRef]
36. Kendall, M.G. *Rank Correlation Methods*, 5th ed.; Oxford University Press: New York, NY, USA, 1990.
37. Healey, J.F. *Statistics: A Tool for Social Research*, 10th ed.; Cengage Learning: Boston, MA, USA, 2014.
38. FAO. *Global Agro-Environmental Stratification (GAES)*; Food and Agriculture Organization of the United Nations: Rome, Italy, 2016.
39. FAO; IIASA. *Global Agro-Ecological Zoning Version 4 (GAEZ v4)*; Available Online at FAO Geospatial; Food and Agriculture Organization of the United Nations: Rome, Italy, 2021.
40. Sayre, R.; Karagulle, D.; Frye, C.; Boucher, T.; Wolff, N.H.; Breyer, S.; Wright, D.; Martin, M.T.; Butler, K.; Van Graafeiland, K.; et al. An assessment of the representation of ecosystems in global protected areas using new maps of World Climate Regions and World Ecosystems. *Glob. Ecol. Conserv.* **2020**, *21*, e00860. [CrossRef]
41. Skalsky, R.; Tarasovicov, Z.; Balkovic, J.; Schmid, E.; Fuchs, M.; Moltchanova, E.; Kindermann, G.; Scholtz, P.; McCallum, I. Global Homogeneous Response Units. *PANGAEA* 2012. [CrossRef]
42. Gregorio, A.D.; Henry, M.; Donegan, E.; Finegold, Y.; Latham, J.; Jonckheere, I.; Cumani, R. *Land Cover Classification System*; Technical Report; FAO: Rome, Italy, 2016.
43. Pérez-Hoyos, A.; Rembold, F.; Kerdiles, H.; Gallego, J. Comparison of Global Land Cover Datasets for Cropland Monitoring. *Remote Sens.* **2017**, *9*, 1118. [CrossRef]
44. George Grekousis, G.M.; Kavouras, M. An overview of 21 global and 43 regional land-cover mapping products. *Int. J. Remote Sens.* **2015**, *36*, 5309–5335. [CrossRef]
45. European Space Agency. *ESA Climate Change Initiative Land Cover Dataset*; European Space Agency: Paris, France, 2023.
46. Mosca, N.; Di Gregorio, A.; Henry, M.; Jalal, R.; Blonda, P. Object-Based Similarity Assessment Using Land Cover Meta-Language (LCML): Concept, Challenges, and Implementation. *IEEE J. Sel. Top. Appl. Earth Obs. Remote Sens.* **2020**, *13*, 3790–3805. [CrossRef]
47. *ISO 19144-2:2023*; Geographic Information—Classification Systems—Part 2: Land Cover Meta Language (LCML). International Organization for Standardization: Geneva, Switzerland, 2023.
48. Mushtaq, F.; Henry, M.; O'Brien, C.D.; Di Gregorio, A.; Jalal, R.; Latham, J.; Muchoney, D.; Hill, C.T.; Mosca, N.; Tefera, M.G.; et al. An International Library for Land Cover Legends: The Land Cover Legend Registry. *Land* **2022**, *11*, 1083. [CrossRef]
49. IPCC. *2006 IPCC Guidelines for National Greenhouse Gas Inventories*; IGES: Hayama, Japan, 2006.
50. Khan, M.Z.; Shoumik, B.A.A. Land degradation neutrality concerns in Bangladesh. *Soil Secur.* **2022**, *9*, 100075. [CrossRef]
51. Jalal, R.; Mahamud, R.; Arif, M.T.A.; Ritu, S.; Kumar, M.F.; Ahmed, B.; Kabir, M.H.; Rana, M.S.; Huda, H.N.; DeGaetano, M.; et al. Restoring Degraded Landscapes through an Integrated Approach Using Geospatial Technologies in the Context of the Humanitarian Crisis in Cox's Bazar, Bangladesh. *Land* **2023**, *12*, 352. [CrossRef]
52. Mamun, A.A.; Islam, A.R.M.T.; Alam, E.; Pal, S.C.; Alam, G.M.M. Assessing Riverbank Erosion and Livelihood Resilience Using Traditional Approaches in Northern Bangladesh. *Sustainability* **2022**, *14*, 2348. [CrossRef]
53. Freihardt, J.; Frey, O. Assessing riverbank erosion in Bangladesh using time series of Sentinel-1 radar imagery in the Google Earth Engine. *Nat. Hazards Earth Syst. Sci.* **2023**, *23*, 751–770. [CrossRef]
54. Olagunju, T.E. Drought, desertification and the Nigerian environment: A review. *J. Ecol. Nat. Environ.* **2015**, *7*, 196–209. [CrossRef]
55. National Directorate of Land-Use Planning—Ministry of Housing, Land Planning and Environment (DINOT-MVOTMA). *Land-Cover Map of Uruguay*; Technical Report (In Spanish); National Directorate of Land-use Planning—Ministry of Housing, Land Planning and Environment (DINOT-MVOTMA): Montevideo, Uruguay, 2014.